Journal of Thermal Analysis and Calorimetry, Vol. 56 (1999) 183-189

SYNTHESIS OF IRON OXIDES BY CO_2 LASER *VS.* THERMALLY INDUCED DECOMPOSITION OF INORGANIC SALTS

C. Popescu[1*], *I. Voicu*[2], *R. Alexandrescu*[2], *I. Morjan*[2], *D. Dumitras*[2], *M. Popescu*[3] *and D. Fatu*[4]

[1]LACECA Research Centre, Str. Siret 95, RO-78308, Bucharest
[2]Institute of Atomic Physics, P.O. Box MG-36, Magurele-Bucharest
[3]CHIMOPAR SA, Bd. Th. Pallady 50, Bucharest
[4]Department of Chemistry, University of Bucharest, Bd. Elisabeta 4-12, Romania

Abstract

This paper reports on the synthesis of various iron oxides by the IR laser processing of different iron salts. X-ray diffraction techniques were used to characterize the reaction products. Some differences in terms of crystallite size and isotropy between these oxides and those obtained from the same salt by thermal means are described and explained.

Keywords: IR laser, iron oxide, thermal analysis, XRD

Introduction

During recent years, much effort has centred on the production and characterization of iron oxides in consequence of a number of specific features which make these oxides attractive for various uses, e.g. catalysts, pigments, magnetic recordings, sensors, etc. It has been observed that both the synthesis method and the choice of precursors strongly influence the morphology and the stoichiometry of the oxides obtained.

The most common precursors for the preparation of iron oxides are iron salts. As compared to the purely chemical methods for the processing of inorganic salts (thermal decomposition, precipitation, etc.), laser methods are characterized by a strong localized action of the light beam, which imposes specific features on the process [1, 2].

In previous papers relating to metal oxide synthesis by CO_2 laser irradiation of inorganic salts [3, 4], we have shown that copper and nickel oxides exhibit peculiarities as concerns their morphology and stoichiometry, these features depending on the absorptivity of the precursors at the wavelength of the laser radiation. The properties were different from those of oxides obtained by conventional controlled heating.

* Author to whom all correspondence should be addressed.

1418–2874/99/ $ 5.00

Akadémiai Kiadó, Budapest
Kluwer Academic Publishers, Dordrecht

In the present work, we report data on the iron oxides obtained by IR laser processing of two iron salts, and discuss the differences revealed by X-ray diffraction techniques between these oxides and those obtained from the same salts by thermal means.

Experimental

Materials

Two iron salts, iron(II) sulphate and iron(III) ammonium alum, were used for the experiments, both of them of analytical purity. Their IR absorbancies are given in Table 1, together with the codes used throughout the paper.

Table 1 IR absorbancy of the iron salts

Iron salt	Absorbancy at 10.6 μm/%
$FeSO_4 \cdot 7H_2O$	14
$FeNH_4(SO_4)_2 \cdot 12H_2O$	31
Fe_2O_3	17
FeO	15

Laser experiments

A cw (continuous wave) CO_2 laser, which produces 10.6 μm radiation, was used to induce the decomposition of the inorganic salts. The laser experiments were performed in an experimental arrangement described elsewhere [5]. The cell containing the inorganic salt undergoing laser treatment was weighed after each passage through the laser beam until its mass was constant. The speed of the cell through the laser beam was 0.3, 0.55 or 1.3 mm s^{-1}, and the power of the laser source was 15, 20 or 25 W.

Thermal experiments

The thermal experiments were conducted in a Derivatograph Q 1500 D (MOM, Budapest). The device records the mass loss (TG) and the thermal effect (DTA curve) when the temperature is changed according to the heating programme from 20 to 1000°C. Air atmosphere, alumina as reference material and a heating rate of 10 or 20°C min^{-1} were used.

X-ray diffraction measurements

The oxide crystals obtained were investigated by means of a Philips diffractometer, with CrK_α radiation in order to measure their size and isotropy.

Results and discussion

On the basis of our previous research [5], we assumed that the decomposition reactions follow the same path during the laser-induced process as during the ther-

Table 2 Reaction steps and the inferred kinetic parameters for thermal and laser-induced decomposition processes

Decomposition reaction stages	Thermal			Laser	
	n	E/kJ mol^{-1}	A/s^{-1}	n	$k(T)$/s^{-1}
$FeSO_4 \cdot 7H_2O$ in thermal regime					
$FeSO_4 7H_2O \rightarrow FeSO_4 \cdot 0.84H_2O + 6.16H_2O$	1	93.2	$3.3\,10^{11}$		
$FeSO_4 0.84H_2O \rightarrow FeSO_4 \cdot 0.72H_2C + 0.12H_2O$	*	*	*		
$FeSO_4 0.72H_2O \rightarrow FeSO_4 \cdot 0.48H_2C + 0.24H_2O$	*	*	*		
$FeSO_4 \cdot 0.48H_2O \rightarrow FeSO_4 + 0.48H_2O$	2/3	259.7	$3.0\,10^{14}$		
$FeSO_4 \rightarrow FeO + SO_3$	*	*	*		
$FeSO_4 \cdot 7H_2O$ in laser regime					
$FeSO_4 \cdot 7H_2O \rightarrow FeO + SO_3 + 7H_2O$				0.61	$4.7 \cdot 10^{-3}$
$FeNH_4(SO_4)_2 \cdot 7H_2O$ in thermal regime					
$2FeNH_4(SO_4)_2 \cdot 12H_2O \rightarrow Fe_2(SO_4)_3 \cdot (NH_4)_2SO_4 + 24H_2O$	1	55.6	$4.5 \cdot 10^6$		
$Fe_2(SO_4)_3 \cdot (NH_4)_2SO_4 \rightarrow Fe_2(SO_4)_3 + 2NH_3 + H_2O + SO_3$	2/3	200.4	$6.4 \cdot 10^{15}$		
$Fe(SO_4)_3 \rightarrow Fe_2O_3 + 3SO_3$	1/3	209.7	$2.0 \cdot 10^{10}$		
$FeNH_4(SO_4)_2 \cdot 7H_2O$ in laser regime					
$2FeNH_4(SO_4)_2 \cdot 12H_2O \rightarrow Fe_2O_3 + 2NH_3 + 4SO_3 + 24H_2O$				0.09	2.37

*The kinetic parameters were not calculated because the resolution of the process in the TG curve did not allow it

mally induced process, and that one of the basic differences between the two types of processes is due to the high heating rates which develop within the impact area of the laser beam. In other words the laser-induced decomposition may be modelled to a good approximation as a fast thermally induced decomposition.

The thermally induced decomposition curves were recorded by the Derivatograph as TG curves. These indicate that there are five different steps through which the iron(II) salt decomposes to FeO, and only three different stages by which the alum decomposes Fe_2O_3. Table 2 gives the reaction steps which occur, according to the recorded mass loss, for the two iron salts. Kinetic analysis of each of the identified steps was performed by using an integral method discussed previously, within the framework of the reaction order [2]. The kinetic parameters (the activation energy, E, the pre-exponential factor, A, and the reaction order, n) were calculated for each step. The values obtained are also given in Table 2.

The mass loss recorded during the laser experiments, for each passage through the laser beam of the cell, indicates decomposition in one step only. As previously assumed, this step is the result of overlapping of five (sulphate) and three (alum) steps recorded during the thermal experiments. This phenomenon of overlapping may be explained by the high heating rate that develops within the laser impact area. An equation was derived earlier to relate the shift in the temperature of the maximum reaction rate from T_{m1} to T_{m2} when the heating rate is changed from β_1 to β_2 [6]:

$$\ln(\beta_2/\beta_1) = E/R(1/T_{m1} - 1/T_{m2}) \quad (1)$$

For a heating rate of about 10^4 °C min^{-1} within the laser beam impact area, one may calculate the temperature of the maximum reaction rate during the laser experiments. The results are given in Table 3.

Table 3 Temperatures of maximum rate, T_m, for the reactions from Table 2 when the heating rate, β, is of the order of 10^4 °C min^{-1}

Reaction		T_m (β=10^4 °C min^{-1})	
		measured	calculated
Iron(II) sulphate	reaction (1)	459	690
	reaction (4)	678	797
Iron(III) sulphate	reaction (1)	428	767
	reaction (2)	630	770
	reaction (3)	825	1065

It can be seen that the calculated temperatures are almost within the same range for iron(II) sulphate and iron(III) alum, demonstrating that all the steps occur almost simultaneously. This may explain why an apparent one-step decomposition reaction is recorded during the laser experiments.

The kinetic analysis of the laser-induced processes should take into account that, during the laser experiments, we measured the mass after the salt had passed through the laser beam. Accordingly, it may be considered that the mass recording was carried out under quasi-isothermal conditions. The integral form of the reaction rate can therefore be re-written:

$$\int_0^{\alpha} \frac{dx}{f(x)} = A\exp\left(-\frac{E}{RT_1}\right)\int_{t_0}^{t} dt \tag{2}$$

where α is the conversion degree, T_1 is the temperature recorded within the laser beam impact area, t_0 is the time at the beginning of the reaction and t is the time at the moment of the weighing. The time interval $(t-t_0)$ may be calculated by considering the number, N, of passes through the laser beam of the cell of length l, with speed v, as given by the following equation:

$$t - t_0 = (Nl)/v \tag{3}$$

If the reaction order model is used again, with substitution of Eq. (3) into Eq. (2), followed by logarithmization and re-arrangement, this becomes

$$\ln[(1-(1-\alpha)^{1-n})/(1-n)] = \ln(N) + \ln(l/v) + \ln[k(T_1)] \tag{4}$$

where $k(T_1)=A\exp(-E/RT_1)$, is the rate constant at the temperature of the experiment. From Eq. (4), one may estimate, to a certain approximation, the values of n and $k(T_1)$. The calculated values, which have informatory rather than kinetic meaning, are listed in Table 2.

The end-products obtained in the two types of experiments were analysed by XRD in order to compare the crystallite sizes and isotropy. We consider this isotropy to be related to the difference between the value of D_{104}/D_{011} and unity.

Effects of experiment type on oxide crystallites

The values of D_{011} and D_{104} for the oxides obtained by the laser and thermal routes are shown in Fig. 1.

It can be seen that the laser experiments produced larger and more anisotropic crystallites than those obtained by the thermal methods. This is in full agreement with our results concerning nickel and copper oxides [3, 4], which showed that the final oxides differ from those obtained by thermal means, provided that the initial salt displays a significant absorbancy of laser radiation. Both of the iron salts absorb well within the range of 10.6 μ, and the results confirm our previous finding [4].

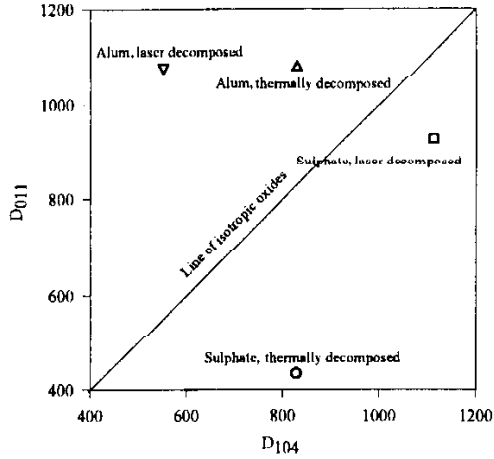

Fig. 1 Oxide crystallite size

Effects of the laser energy

The influence of the laser-supplied energy on the crystallites obtained was also investigated earlier [3]. From the definition of energy:

$$W = Pt \tag{5}$$

where W is the energy and P is the laser power, by replacing time t via Eq. (3) and rearrangement we obtain

$$\frac{W}{l} = \frac{NP}{\nu} \tag{6}$$

Equation (6) reveals a linear relationship between the energy supplied per unit length and the ratio P/ν, of two parameters we may control. The influence of the energy supplied by the laser on the physical form of the end-product may be investigated by modifying the laser power and the speed of the cell through the laser beam, whilst keeping the number of passages, N, constant. Table 4 shows the dependence of the dimensions D_{104} and D_{011} on the value of P/ν for a constant number of passages, N=2.

Table 4 demonstrates that the crystallite size is dependent on the energy supplied, which in turn is related to the absorbancy of the initial salt decomposed.

These experiments show that the use of laser decomposition to produce iron oxides again indicates the influence of the initial salt absorbancy value on the final physical form of the oxide obtained. We have termed this phenomenon the 'laser ef-

Table 4 Influence of *P*/v on oxide crystallite size (Å)

P/v	Iron(II) sulphate		Iron(III) alum	
	D_{011}	D_{104}	D_{011}	D_{104}
19.23	509.7700	216.6900	463.4466	661.9425
27.27		552.3100	295.0713	472.4714
36.36	927.9300		463.6361	413.8003
50.00		828.2000	811.6119	662.2875
66.66	812.0260	1104.5000	1081.7000	472.7175
83.33	1082.7000	828.3700	1081.4860	661.8045

fect', and our data reveal that it is related to the value of *P*/v: the higher the value of *P*/v, the larger the crystallites obtained (Table 4).

Conclusions

The kinetic analysis of the decomposition of these iron salts by laser and thermal means demonstrates that a controlled heating process occurs in several steps, with intermediates which may be identified, whereas the laser induced process takes place in a single step, with the oxide as only final compound. This can be explained by assuming that the laser is a very rapid heating source, with high temperatures developing within the laser beam impact area. Consequently, the temperatures of all the intermediate steps are compressed within the same temperature range, in good agreement with the calculations performed in connection with Eq. (1).

The iron oxide crystallites produced by laser-assisted decomposition are larger and more anisotropic than those obtained by controlled heating. This result is in good agreement with our previous studies with nickel and copper oxides [3, 4], and reinforces what we have named the 'laser effect'. This describes the relationship between the absorbancy properties of the initial salt and the size of the crystallites produced by laser heating.

References

1 E. Borsella, S. Botti, M. Cesile, S. Martelli, R. Alexandrescu, R. Giorgi, C. A. Nametti, S. Turtu and G. Zappa, Nanostructured Materials, 6 (1995) 341.
2 R. Alexandrescu, R. Cireasa, B. Dragnea, I. Morjan, I. Voicu, A. Andrei, F. Vasiliu, C. Popescu and D. Fatu, Advanced Mat. Optics Electronics, 5 (1995) 19.
3 C. Popescu, D. Fatu, R. Alexandrescu, I. Voicu, I. Morjan, M. Popescu and V. Jianu, J. Mater. Res., 9 (1994) 1257.
4 R. Alexandrescu, C. Popescu, I. Morjan, I. Voicu and D. Dumitras, Infrared Phys. Technol., 36 (1995) 1.
5 C. Popescu, R. Alexandrescu, I. Morjan and M. Popescu, Thermochim. Acta, 184 (1991) 73.
6 C. Popescu and E. Segal, Thermochim. Acta, 82 (1984) 387.